Modeling self-heating in high-power non-circular VCSELs

Modeling self-heating in high-power non-circular VCSELs

M. C. G. Alasio[1], V. Torrelli[1,2], S. Albano[1], L. Miri[1], A. Gullino[2], M. Goano[1,2] and P. Debernardi[2]

1. Department of Electronics and Telecommunications (DET), Politecnico di Torino, Italy

2. Istituto di Elettronica e di Ingegneria dell'Informazione e delle Telecomunicazioni (IEIIT) del Consiglio Nazionale delle Ricerche (CNR), Politecnico di Torino, Italy

matteo.alasio@polito.it

***Abstract*— VCSEL applications are continuously growing, especially in sensing. High-power, *i.e.*, large area, and single-mode are contradictory requirements, tackled by mastering VCSEL temperature distribution (TD) and proper design. We present here a viable approach aimed at efficiently introducing TD in 3D simulations of optical modes.**

Keywords—VCSELs, self-heating, temperature, high-power

I. Introduction

In addition to their known use in datacom, vertical-cavity surface-emitting lasers (VCSELs) are also employed for sensing or optical pumping. For example, quantum gyroscopes and atomic clocks necessitate emission that is both high-power and single-mode [1,2]. Large active area (LAA) devices, such as rectangular VCSELs [3,4], feature multi-mode emission, which can be converted into single mode, by proper surface patterning. To this end, a series of grating reliefs can be etched on the outcoupling facet of LAA-VCSELs. These reliefs must be aligned with the specific transverse mode that is intended for single-mode emission [1]. Such a line-up is significantly influenced by the operating current, resulting in an increase in temperature due to self-heating. This leads to thermal lensing and further confinement of the modes, altering the alignment. Accurate understanding of the temperature distribution within LAA-VCSELs is crucial for effective relief array design. The temperature variation distribution can be translated into a modification of refractive index, which can be plugged into optical solvers to determine single mode performances [1,5].

In this work, we focus on modeling the self-heating temperature profile T, using experimental light-current (LI), current-voltage (IV) and spectral intensity data presented in [3] for various rectangular VCSELs. In addition, we extract analytic elliptical shapes for the T contour lines, useful for computationally efficient mode solvers [5].

II. Model and Results

To model the self-heating temperature profile in VCSELs, the heat equation must be solved by including a comprehensive heat source, reading

$$\nabla \cdot (\kappa \nabla T) = -Q, \tag{1}$$

where κ represents the VCSEL thermal conductivity, with values reported in Tab. 1.

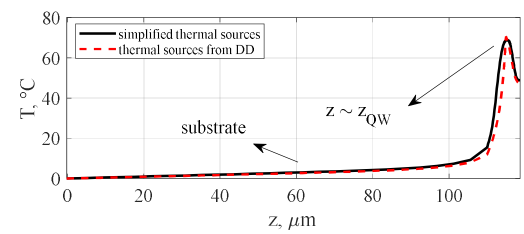

Fig. 1. Self-heating temperature profile along the longitudinal direction z for a conventional circular VCSEL using both the actual thermal sources from [6,7] and the simplified source define in (2).

Q is generally the sum of different contributions. To mention only the most relevant terms: the Joule heating, recombination rates obtained from a drift-diffusion (DD) solver, and quantum-well capture heating, self-consistently coupled with optical modes [6,7]. Aiming at an extensive simulation campaign on VCSELs with different geometries, we use and test a simplified thermal source, based on the knowledge of LI and IV data. Indeed, we may consider a piece-wise constant source, defined as

$$Q = \frac{P_{\mathrm{loss}}}{V}, \tag{2}$$

where $P_{\mathrm{loss}} = V_{\mathrm{bias}} I_{\mathrm{bias}} - P_{\mathrm{opt}}$ is the dissipated thermal power, P_{opt} the optical power, while V is the volume associated to the constant source. The source is transversely defined by the oxide aperture and vertically placed at the quantum wells (QWs).

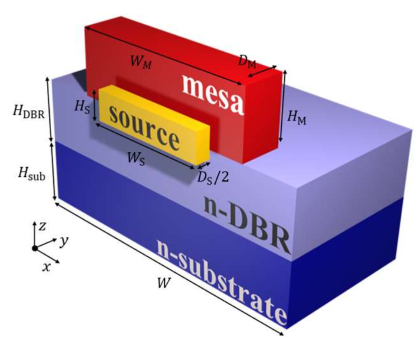

Fig. 2. Perspective view of the simulation domain and the simplified heat source with important geometrical quantities reported. The mesa is encapsulated within a passivation layer, not shown in the figure.

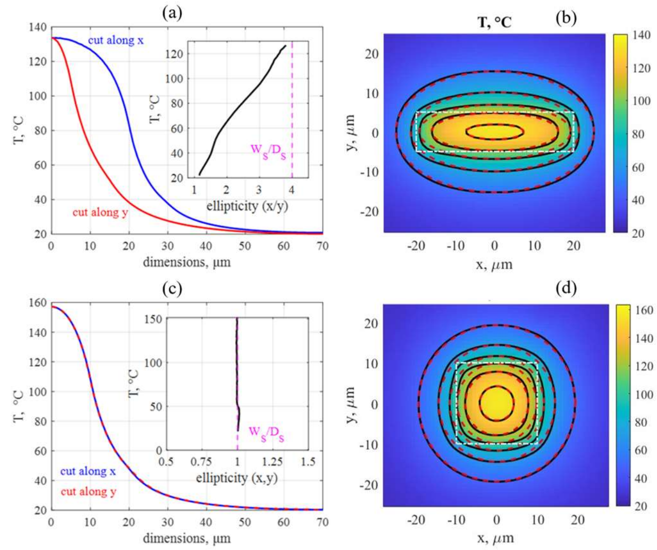

Fig. 3. (a), (c): self-heating temperature profile cuts at the QWs section along the x (blue) and y (red) directions. Insets represent the x-to-y ratios of such cuts, which can be interpreted as the ellipticity of isothermal contours. Magenta dashed lines represent the aspect ratio of the oxide aperture. (b), (d): color map and contour plot (black solid lines) of the self-heating temperature at the QWs section, with the analytical ellipses (dashed red lines). White dashed lines represent the oxide aperture.

The simplified thermal source is applied to the conventional circular VCSEL whose structure is described in [6,7], showing that the self-heating temperature profile is properly reproduced with a thickness of the thermal source of 4 µm, as reported in Fig. 1. This methodology can now be extended with a finite element method (FEM) to 850 nm *pin* rectangular structures, as the one reported in Fig. 2. In the three simulated structures inspired by [3], we consider $H_{\mathrm{sub}} = 120$ µm, $H_{\mathrm{DBR}} = 6.7$ µm, $H_{\mathrm{M}} = 2$ µm, $W_{\mathrm{M}} = W_{\mathrm{S}} + 20$ µm, $D_{\mathrm{M}} = D_{\mathrm{S}} + 20$ µm, with W_{S} and D_{S} representing the oxide aperture, and consequently the source size, for all the variants.

As a validation, the first case with $W_{\mathrm{S}} = 125$ µm and $D_{\mathrm{S}} = 5$ µm was simulated with substrate size $W = 240$ µm. Indeed, the experimental spectral intensity data allow to crosscheck the computed temperature profile.

At rollover $P_{\mathrm{loss}} \sim 200$ mW, the wavelength shift is $\Delta\lambda \sim 5$ nm and the emission wavelength is $\lambda \sim 860$ nm [1]. By recalling that the refractive index variation rate with temperature, dn/dT, is linked to the self-heating temperature rise T and wavelength shift according to [7] as

TABLE I.

Layer	**κ, Wm^{-1}(°C)$^{-1}$**
substrate	46
DBRs, active region and mesa (transverse)	15
DBRs, active region and mesa (longitudinal)	12
passivation	0.5

$$\frac{dn}{dT} = \frac{\bar{n}}{\lambda}\frac{\Delta\lambda}{T}, \tag{3}$$

we infer from the computed temperature rise $T \sim 85$ °C a $\frac{dn}{dT} \sim 2.22 \cdot 10^{-4}$ (°C)$^{-1}$, in accordance with typical values for 850 nm VCSELs [7].

Second and third structures present lower aspect ratios, thus allowing a lower number of FEM mesh points and reducing the computational time. Specifically, a rectangular structure with $W_{\mathrm{S}} = 40$ µm and $D_{\mathrm{S}} = 10$ µm and a square structure with $W_{\mathrm{S}} = D_{\mathrm{S}} = 20$ µm were simulated with substrate size $W = 140$ µm, resulting in an equal area of 400 µm^2. P_{loss} was set for the rectangular case to 135 mW in correspondence of the roll-over point at 66 mA, and 152 mW for the square case to keep the same current.

Results are reported in Fig. 3. The maximum temperature rise for the rectangular case is ~140 °C, lower than the square case at ~160 °C, confirming the experimental trends in [3], for which larger aspect ratios allow for better heat dissipation, thus pushing roll-over towards higher currents. If isothermal contour lines are assumed to be ellipses, the corresponding semi major and minor axes and ellipticity can be estimated for a fixed T by evaluating the corresponding positions along x and y cuts, as done in Fig. 3a and 3c. This assumption is verified by comparing the analytic ellipses with actual contour lines in Fig. 3b and 3d. Both the retrieved self-heating temperature profiles and analytic contour lines serve as input for optical mode solvers, representing the starting point for optimizing the design of relief arrays for single-mode operation.

III. Conclusion

We present an efficient approach to investigate and optimize the temperature self-heating profile in large-area, high-power VCSELs and test it on experimental results, using the observed wavelength shift as a “VCSEL thermometer”. Model and experiments compare very well and allow us to apply it for future design optimization.

ACKNOWLEDGMENTS

Project funded under the National Recovery and Resilience Plan (NRRP), Mission 4, Component C2, Investment 1.1, by the European Union – NextGenerationEU. PRIN Project 20225YYLEP, "Empowering UV Led technologies for high efficiency disinfection: from semiconductor-level research to SARs-Cov-2 inactivation"

References

[1] V. Torrelli, et al., IEEE Photon. J. 16, 0600507 (2024).
[2] M. Xun, et al., IEEE Electron Device Lett. 44, 1144 (2023).
[3] S. Gronenborn, et al., IEEE J. Select. Topics Quantum Electron. 48, 1040 (2012).
[4] S. Gronenborn, et al., Appl. Phys. B 105, 783 (2011).
[5] G. P. Bava, P. Debernardi, L. Fratta, Phys. Rev. A 63, 23816 (2001).
[6] A. Tibaldi, F. Bertazzi, M. Goano, R. Michalzik, P. Debernardi, IEEE J. Select. Topics Quantum Electron. 25, 1500212 (2019).
[7] P. Debernardi, et al., IEEE J. Select. Topics Quantum Electron. 25, 1700914 (2019).